NIH Public Access
Author Manuscript
J Comp Neurol. Author manuscript; available in PMC 2010 May 4.

Published in final edited form as:
J Comp Neurol. 2008 March 20; 507(3): 1300–1316. doi:10.1002/cne.21514.

Comparison of the Distributions of Urocortin Containing and Cholinergic Neurons in the Perioculomotor Midbrain of the Cat and Macaque

Paul J. May[1], **Anton J. Reiner**[2], and **Andrey E. Ryabinin**[3]

[1] Departments of Anatomy, Ophthalmology and Neurology, University of Mississippi Medical Center, Jackson, MS, 39202, U.S.A

[2] Department of Anatomy and Neurobiology, University of Tennessee, Memphis, TN, 38163, U.S.A

[3] Department of Behavioral Neuroscience, Oregon Health Science Center, Portland, OR, 97239, U.S.A

Abstract

Urocortin is a novel neurotransmitter that appears to play a role in eating and drinking behavior. Most urocortin-positive (urocortin$^+$) neurons in rodents are found in the cytoarchitecturally defined Edinger-Westphal nucleus (EW). However, the EW is traditionally described as the source of the preganglionic parasympathetic outflow to the ciliary ganglion. We examined the distribution of urocortin$^+$ cells and motoneurons by use of immunohistochemical staining for this peptide and for choline acetyl transferase (ChAT) in macaque monkeys, where most preganglionic motoneurons inhabit the EW, and in cats, where most do not. In both species, lack of overt double labeling indicated the ChAT$^+$ and urocortin$^+$ cells are separate populations. In the monkey, most non-oculomotor ChAT$^+$ neurons were found within the EW. In contrast, urocortin$^+$ cells were mainly distributed between the oculomotor nuclei, and in the supraoculomotor area. In the cat, most non-oculomotor ChAT$^+$ cells were located in the supraoculomotor area and anteromedian nucleus. Few were present in the cat EW. Instead, this nucleus was filled with urocortin$^+$ cells. These results highlight the fact the term EW has come to indicate different nuclei in different species. Consequently, we have adopted the identifiers preganglionic (EW_{PG}) and urocortin containing (EW_U) to designate the cytoarchitecturally defined EW nuclei in monkeys and cats, respectively. Furthermore, we propose a new open-ended nomenclature for the perioculomotor (pIII) cells groups that have distinctive projections and neurochemical signatures. This will allow more effective scientific discourse on the connections and function of groups like the periculomotor urocortin ($pIII_U$) and preganglionic ($pIII_{PG}$) populations.

Indexing Terms

Edinger-Westphal; Oculomotor; Preganglionic Parasympathetic; Appetite; Stress; Lens; Pupil

INTRODUCTION

The peptide urocortin, a novel putative neuropeptide transmitter, was initially detected in neurons located in the midbrain of rodents (Vaughan et al., 1995; Kozicz et al., 1998;

Corresponding Author: Paul J. May, PhD, Department of Anatomy, University of Mississippi Medical Center, 2500 North State St., Jackson, MS, 39216, USA, Phone # 601-984-1662, FAX # 601-84-1655, pmay@anatomy.umsmed.edu.

NIH-PA Author Manuscript
NIH-PA Author Manuscript
NIH-PA Author Manuscript

NIH-PA Author Manuscript

NIH-PA Author Manuscript

NIH-PA Author Manuscript

Yamamoto et al., 1998). Other locations in the brain, including the lateral superior olive and supraoptic nucleus, have also been shown to contain urocortin positive cells, but the rostral midbrain contains the largest population (Bittencourt et al., 1999; Lim et al., 2006; Morin et al., 1999; Weitemier et al., 2005). Urocortin is structurally similar to corticotropin-releasing factor (CRF), which is a well-known mediator of stress responses and anxiety (Heinrichs and Richard, 1999; Vale et al., 1981; Vaughan et al., 1995). Further CRF- related compounds have since been isolated, which are designated as Urocortin 2 and 3, with the original urocortin designated Urocortin 1 (Hauger et al., 2003; Bale and Vale, 2004). Here we examined Urocortin 1, which for purposes of simplicity will be designated as just urocortin in this report. Urocortin is able to activate both CRF_1 and CRF_2 receptors, and it binds to these receptors and CRF binding protein more readily than CRF itself (rat: Vaughan et al., 1995). In fact, urocotin levels have been found to have an inverse relationship to CRF levels (mouse: Kozicz et al., 2004; Weninger et al., 2000; rat: Skelton et al., 2000). This may have important medical consequences, as both CRF and urocortin levels have been associated with stress (rat: Gaszner et al., 2004; Kozicz et al., 2001; mouse: Weninger et al., 2000). Urocortin and CRF also seem to play a role in appetite control (Heinrichs and Richard, 1999; Spina et al., 1996). This includes appetite for drugs and alcohol, as well as food. For example, the level of expression of urocortin in midbrain urocortin-positive neurons has been tied to the propensity for alcohol consumption, and this same set of neurons shows up-regulation of c-fos expression in response to alcohol intake (mouse: Bachtell et al., 2002; 2003). Taken together, these studies suggest that the urocortin system in the rostral midbrain, like the serotonergic one in the caudal midbrain, may play a role in modulating several important behaviors. Moreover, there is a fairly limited distribution of urocortin-positive cells that give rise to a widespread distribution of urocortin-positive terminals, a pattern like that of the dorsal raphe (monkey: Vasconcelos et al., 2003; mouse: Weitemier et al., 2005; rat: Bittencourt et al., 1999).

The main population of urocortin-positive cells has been described as lying in the Edinger-Westphal nucleus (EW) of the rodent midbrain, as these cells are found in a region of closely packed neurons located on either side of the midline between the oculomotor nuclei (mouse: Bachtell et al., 2002; rat: Kozicz et al., 1998; Yamamoto et al., 1998; vole: Lim et al, 2006). However, the names Edinger and Westphal have long been associated with the cells of origin of the parasympathetic outflow that travels via the third cranial nerve, and supplies the ciliary ganglion for control of the ciliary and pupillary sphincter muscles (Edinger, 1885; Westphal, 1887). Edinger described the presence of groups of smaller neurons associated with the oculomotor nucleus, and Westphal described a clinical case in which extraocular function was lost, but pupillary constriction and lens accommodation were maintained. In this case, pathological examination showed a lesion that involved the large celled portions of the oculomotor nucleus, but preserved the smaller cells located more dorsally. Contemporary retrograde tracer studies in old and new world monkeys have demonstrated that the preganglionic parasympathetic motoneurons supplying the ciliary ganglion lie in two columns of cells that are located dorsal to the oculomotor nucleus on either side of the midline (Akert et al., 1980; Burde and Loewy, 1980, Clarke et al., 1985). The vast majority of these cells lie in a cytoarchitecturally distinct nucleus within the monkey midbrain, which has been termed the EW. The column of preganglionic motoneurons extends rostrally further than the oculomotor nucleus, where it occupies a portion of the anteromedian nucleus (Akert et al., 1980; May et al., 1992). Physiological investigations of the neurons in the monkey EW demonstrate that their firing rates are correlated with the activity of the ciliary and sphincter pupillae muscles (Gamlin et al., 1994), and electrical stimulation of EW produces lens accommodation and pupillary constriction (Crawford et al., 1989; Vilupuru and Glassner, 2005). The distribution of these preganglionic motoneurons in prosimian primates is similar to that of monkeys (Sun and May, 1983). In birds as well, the EW is the source of the preganglionic outflow to the ciliary ganglion (Gamlin and Reiner, 1991; Reiner et al., 1983; 1991), although the bird EW also has been shown to regulate blood flow in the choroid, in

NIH-PA Author Manuscript

NIH-PA Author Manuscript

NIH-PA Author Manuscript

addition to producing pupillary constriction and lens accommodation (Fitzgerald et al., 1990, 1996). On the other hand, Ryabinin and colleagues (2005) have recently demonstrated that the cytoarchitecturally defined nucleus traditionally termed the Edinger-Westphal nucleus in humans (Olszewski and Baxter, 1982) contains primarily urocortin-positive neurons, not neurons that are immunoreactive for choline acetyl transferase (ChAT).

In non-primate mammals, the organization of the oculomotor preganglionic motoneurons is more diffuse. For example, cats display a midline nucleus located immediately dorsal to the oculomotor nucleus, which has been called the EW. Surprisingly, only a small portion of the preganglionic motoneurons supplying the ciliary ganglion are located within this nucleus. The rest are found in the supraoculomotor area (SOA), along the midline between the oculomotor nuclei, in and around the anteromedian nucleus, and among the exiting rootlets of the oculomotor nerve, just beneath the medial longitudinal fasciculus (MLF) (Erichsen and May, 2002; Loewy and Saper, 1978; Loewy et al., 1978; Sugimoto et al., 1977; Toyoshoma et al., 1980). In contrast, the cytoarchitecturally defined EW of the cat appears to be the source of projections to a variety of central structures, including the cerebellum and spinal cord (Loewy and Saper, 1978; Loewy et al., 1978; Røste and Dietrichs, 1988a&b; Sugimoto et al., 1978). In addition, these centrally projecting cells appear to be peptidergic and have been reported to show immunoreactivity for substance P, cholecystokinin (CCK) and even CRF (Chung et al., 1987; Maciewicz et al., 1983; 1984). [More recently, it was suggested that the immuoreactivity for CRF in EW can be attributed to cross-reactivity with urocortin, because CRF mRNA expression is not found there (rat: Bittencourt et al., 1999)] In rabbit, the preganglionic motoneurons are largely found among the exiting third nerve rootlets, beneath the oculomotor nucleus (Johnson and Purves, 1981). The organization in rodents is less well understood, as the small size of the ciliary ganglion makes it a difficult injection target. Inoculations of the anterior chamber with pseudorabies virus, a trans-neuronal retrograde marker, have been employed in rodents to overcome this difficulty (mouse: Vann and Atherton, 1991; rat: Smeraski et al., 2004). These studies suggest the preganglionic motoneurons are mainly located in the area of the anteromedian nucleus. Rodents also have a nucleus designated as EW. It is a small, paired nucleus located on either side of the midline, between the oculomotor nuclei in mouse (Paxinos and Franklin, 2001), and has a slightly more dorsal location in rat (Paxinos and Watson, 1982).

Working under the assumption that the preganglionic parasympathetic neurons should be positive for antibodies to choline acetyl transferase (ChAT), Weitemier and colleagues (2005) have recently demonstrated that the urocortin-positive neurons in the mouse EW are not ChAT-positive ($ChAT^+$), and so presumably project centrally, and not to the ciliary ganglion. In view of the possible importance of the urocortin-positive ($urocortin^+$) population of midbrain neurons, it seemed reasonable to determine their location in other species commonly used in neuroscience investigations. Furthermore, the present study was directed at determining the exact relationship of the $urocortin^+$ population with respect to the preganglionic parasympathetic motoneurons supplying the eye, and to the boundaries of the cytoarchitecturally defined EW. In light of these criteria, we chose to investigate the location of $urocortin^+$ and $ChAT^+$ populations in the cat and macaque monkey. These species were chosen both because they have the best studied EW, and because the relationship between the EW and the preganglionic population in these two species is notably different.

METHODS

The methods used in these experiments were approved by the investigator's respective local Institutional Animal Care and Use Committees, and fall within the accepted practices outlined by the NIH Guide for the Care and Use of Animals. The study employed adult cats (n = 5) and monkeys, *Macaca fascicularis* and *mulatta*, (n = 8) of both sexes. The tissue used in the study

NIH-PA Author Manuscript

NIH-PA Author Manuscript

NIH-PA Author Manuscript

was taken from animals that had been employed in chronic physiology experiments and were being sacrificed for routine histology, or were part of other anatomy experiments that would not conflict with the immunohistochemical studies presented here. Before perfusion, the monkeys were sedated with ketamine HCl (10 mg/kg). All animals were anesthetized with an overdose of sodium pentobarbital (50–70 mg/kg, IP). Once they were entirely non-responsive, they were perfused through the heart with a wash consisting of 0.1 M, pH 7.2 phosphate buffered saline (PBS), followed by a fixative solution containing 4 % paraformaldehyde in 0.1 M, pH 7.2 phosphate buffer (PB). The brains were blocked in the frontal plane, *in situ*, then removed and postfixed overnight at 4°C in the same fixative. They were then equilibrated in 30 % sucrose in PB at 4°C as a cryoprotectant. At this point, they were frozen and sectioned on a sliding microtome. The sections (50 or 80 μm) were collected in serial order and stored at 4°C until processed.

To reveal the presence of urocortin containing neurons, a series of sections was first treated with 0.3 % H_2O_2 to eliminate endogenous peroxidase activity, and then placed in a blocking solution consisting of 2.0 % bovine serum albumin (BSA) in 0.1 % Triton X-100 in PBS. The sections were then incubated overnight at 30°C in primary antibody to urocortin at a 1:10,000–15,000 dilution in 0.03 % Triton X-100, 0.1 % BSA, PBS. The urocortin antibody (Sigma-Aldrich, catalog # U4757, lot # 039H4815) was raised in rabbit against amino acids 25–40 of the human peptide. The primary antibody was then tagged with a biotinylated anti-rabbit secondary (Vector Labs), which was in turn revealed using a Vectastain ABC kit (Vector Labs). The chromagen diaminobenzidine was used to visualize the ABC kit horseradish peroxidase tag, in some cases using conventional nickel/cobalt intensification methods (Adams, 1981). The sections were then mounted on slides, counterstained with cresyl violet (in some cases), dehydrated, cleared and coverslipped. To visualize the choline acetyl transferase (ChAT), an antibody to ChAT (Chemicon International, catalog # AB144P, lots 21120024 & 0603026202) raised in goat to human placental enzyme was used at a dilution of 1:480 in a procedure like that described for urocortin, with the exception of the fact a goat ABC kit was employed.

Conventional controls utilizing omission of the primary or secondary antibodies were run for both urocortin and ChAT. These procedures resulted in complete absence of immunohistochemical signal. The Sigma anti-urocortin antibody was controlled for specificity in our previous study, in which preincubation of the primary antibodies with 0.1 mmol of urocortin, but not CRF, urocortin 2 or urocortin 3, abolished the immunohistochemical signal (Bachtell et al., 2003), and recently using the knockout test, in which there was no urocortin-positive staining in urocortin knockout mice (Ryabinin, unpublished observations). The Chemicon anti-ChAT antibody has been also controlled for specificity in previous studies by others. For example, Leger and colleagues (1999) observed that omission of primary antibody or preincubation with a 100-fold excess of appropriate antigens results in lack of immunohistochemical signal.

To simultaneously reveal the location of both the urocortin$^+$ neurons and the cholinergic motoneurons, a sequential fluorescence immunohistochemical procedure was employed with the antibodies listed above. First, the sections were washed in 0.3 % Triton in PBS, and then they were placed in blocking solution consisting of 1% bovine serum albumin (BSA). Next, they were incubated overnight in the first primary antibody, a solution of 1:10,000 rabbit anti-urocortin. After several PBS rinses, they were placed in biotinylated donkey anti-rabbit secondary (1:500 in 0.3 % triton PBS). They were rinsed again, and then placed in Cy2-conjugated (green fluorescing) Streptavidin in Triton/PBS (1:200) (Jackson Labs). To reveal the cholinergic population, the sections were again rinsed in PBS and place in a second primary antibody overnight at 4°C: goat anti-ChAT 1:480 in 1% BSA/Triton/PBS solution. The following morning, they were rinsed and incubated in Cy3- conjugated (red fluorescing) donkey anti-goat IgG (Jackson Labs) at 1:200 in 1% BSA/Triton/PBS. They were then rinsed

NIH-PA Author Manuscript

NIH-PA Author Manuscript

NIH-PA Author Manuscript

a final time in PBS and mounted onto gelatinized slides. Once the mounted sections were completely dry, they were coverslipped using DPX mounting medium for fluorescence microscopy.

Sections from both the single- and double-label procedures were viewed using a Nikon microscope equipped for conventional and fluorescence observation. Images of interest were obtained using a Nikon black and white or a CoolSNAP color digital camera, through the application of Metamorph software. The sequential fluorescence immunohistochemistry images were taken as two individual fluorophore-specific images with the black and white camera. They were then pseudocolored to match the observed view and combined digitally. All images were further adjusted with respect to brightness, contrast and color balance using Adobe Photoshop to best resemble the image seen through the eye pieces. The red channel was then converted to magenta in Photoshop. Chartings of single labeled tissue were made using an Olympus Microscope equipped with a drawing tube, while those of double-labeled tissue were made using a Leica fluorescent microscope with x and y stage digitizers, and the help of dedicated computer hardware and programs (Datametrics).

RESULTS

Macaque

The appearance and distribution of urocortin$^+$ neurons in the macaque can be appreciated in figure 1B&D. A number of urocortin$^+$ neurons are located along the midline, between the oculomotor nuclei. However, the majority of these cells are found above the oculomotor nucleus within the supraoculomotor area. There they avoid the midline, and instead fan out dorsolaterally. The size of the cells appears to increase slightly as they extend dorsolaterally. A few urocortin$^+$ cells are also present further laterally, among the fascicles of the medial longitudinal fasciculus (MLF) and in the adjacent midbrain reticular formation (MRF). Comparison of the distribution of the urocortin$^+$ population to the ChAT$^+$ population (Fig. 1A&C) shows distinct differences in distribution. ChAT$^+$ cells, presumably extraocular motoneurons, dominate the oculomotor nucleus. A group of smaller ChAT$^+$ neurons is found along the medial and dorsal edges of the oculomotor nuclei (Fig. 1C, arrowheads). These are presumably the S- and C-group motoneurons that supply the multiply innervated muscle fibers within the extraocular muscles (Büttner-Ennever and Akert, 1981; Eberhorn et al., 2005). ChAT$^+$ positive cells are also found in two clusters dorsal to the oculomotor nucleus. These represent the cholinergic preganglionic motoneurons of the Edinger-Westphal nucleus (EW). While the urocortin$^+$ cells are clearly not confined to EW, it was uncertain from urocortin-immunolabeled material whether or not some urocortin$^+$ cells are, in fact, located within its boundaries.

The overall distribution of the urocortin$^+$ cells with respect to cytoarchitectonic boundaries defined by counterstaining these sections is illustrated for the macaque in figure 2. Rostrally (Fig. 2A–C), numerous urocortin$^+$ cells are present in the anteromedian nucleus (AM), although they spill out dorsal and rostral to the boundaries of this nucleus. At the level of the oculomotor nucleus (Fig. 2D–H) urocortin$^+$ cells are found on the midline between the dorsal halves of the oculomotor nuclei, and distribute dorsolaterally into the SOA. Only a few urocortin$^+$ cells are found within the confines of EW. At rostral levels of the oculomotor nucleus (Fig. 2D&E), this population spills out into the periventricular gray, interstitial nucleus of Cajal (InC) and the MRF adjacent to the MLF. Caudally (Fig. 2F–H), these cells are found among the bundles of MLF fibers and in the adjacent MRF.

Dual immunofluorescence experiments provided further insight into the relative location of the urocortin$^+$ and ChAT$^+$ populations. As shown in figure 3, the magenta fluorescing ChAT$^+$ cells are again found either in or adjacent to the oculomotor nucleus proper, or in two

NIH-PA Author Manuscript

NIH-PA Author Manuscript

NIH-PA Author Manuscript

clusters located on either side of the midline, dorsal to the oculomotor nucleus, in the location of the EW (Fig. 3A&B). Green fluorescing urocortin$^+$ cells are found in a narrow band along the midline, between the oculomotor nuclei, and then wrapping dorsolaterally, in the supraoculomotor area dorsal to the oculomotor nucleus. They are not found medially in the supraoculomotor area. A few urocortin$^+$ cells are found among the ChAT$^+$ motoneurons of the oculomotor nucleus (Fig. 3A). In addition, urocortin$^+$ cells are scattered in the MLF lateral to the SOA and in the MRF lateral to the MLF (Fig. 3B). With respect to the EW, there was overlap in the distributions of the urocortin$^+$ cells and the ChAT$^+$ preganglionic motoneurons along its lateral edge (Fig. 3A&C). There was also some overlap in the distribution of urocortin$^+$ cells and the small ChAT$^+$ cells of the C- and S-groups (Fig. 3A, arrowheads). However, there were no cells showing a yellow color, indicative of staining by both antibodies and thus co-localization of ChAT and urocortin in the same neuron, either within the EW or elsewhere in the perioculomotor area.

The total distribution of the two fluorescent populations can be better appreciated in the chartings of figure 4. ChAT$^+$ motoneurons fill the oculomotor nucleus proper, extending into the MLF (Fig. 4D–I), as well as the caudal central subdivision (Fig. 4I). In addition, ChAT$^+$ cells, presumably preganglionic motoneurons, are found in two columns above the oculomotor nuclei proper, beginning in front of the caudal central subdivision (Fig. 4H) and extending rostrally above the oculomotor nucleus (Fig. 4D–H). The rostral pole of this group lies within the middle portion of the AM nucleus (Fig. 4A–C). In contrast to the ChAT$^+$ cells, the urocortin$^+$ cells fill the entirety of the AM nucleus, and extend beyond its borders (Fig. 4A–C). At levels containing the oculomotor nucleus (Fig. 4D–H), they wrap around the oculomotor nucleus proper, so that they are found medial to it, dorsal to it in the supraoculomotor area and periaqueductal gray, and lateral to it in the MLF and adjacent reticular formation. This population ends at the level of the caudal central subdivision (Fig. 4I), and is not present more caudally, where the serotonergic neurons of the dorsal raphe take up this midline position.

Feline

The appearance and distribution of urocortin$^+$ cells in the cat midbrain can be appreciated in figure 5. In the cat, the majority of urocortin$^+$ cells reside within the nucleus that has been termed the EW in this species (Fig. 5A&B). In frontal sections through the oculomotor nucleus, the cat EW forms a single, heart-shaped domain on the midline above the oculomotor nucleus proper. Urocortin$^+$ cells extend ventrally from the EW, between the two oculomotor nuclei. In addition, a few urocortin$^+$ cells are scattered within the SOA, and laterally into the MRF (Fig. 5A). The urocortin$^+$ population extends rostral to the oculomotor nucleus within the AM, and even rostral to the AM. In front of the AM, it forms two cell columns, centered off the midline, in the central gray beneath the third ventricle (Fig. 5C&D).

The overall distribution of urocortin$^+$ cells in the cat is illustrated in figure 6. Rostral to EW, the AM nucleus contains urocortin$^+$ neurons (Fig. 6C). The beginnings of two urocortin$^+$ rostral columns are evident ventrolateral to the AM at this level. Rostral to this level (Fig. 6A&B), these paired columns are located just off the midline. At the level of the oculomotor nucleus (Fig. 6D–H), the vast majority of urocortin$^+$ neurons are located within the cat EW. However, positive neurons are also apparent ventrally, between the oculomotor nuclei, in the SOA, and in the MLF and adjacent midbrain reticular formation.

To better discriminate whether the oculomotor and preganglionic motoneurons formed a separate population with respect to the urocortin$^+$ population in the cat, we utilized combined immunofluorescence for urocortin and ChAT in the same sections. Results from these experiments are shown in figure 7. The green (Cy-2 labeled) urocortin$^+$ population is primarily located in the EW (Fig. 7C&D), although a few urocortin$^+$ neurons extend down from EW between the oculomotor nuclei. In addition, a few scattered cells are found in the SOA (Fig.

NIH-PA Author Manuscript

NIH-PA Author Manuscript

NIH-PA Author Manuscript

7D, arrowhead) and in the midbrain reticular formation (Fig. 7C, arrowhead). In contrast, the magenta (Cy-3 labeled) ChAT$^+$ neurons are primarily found in the oculomotor nucleus proper (Fig. 7C&D). The scattered ChAT$^+$ neurons located outside of this nucleus represent presumed preganglionic motoneurons. Many of these are found in the SOA. The extension of these two populations rostral to the oculomotor nucleus can be seen in figure 7A&B. Here the green fluorescing urocortin$^+$ cells are primarily found in AM, although scattered neurons are present laterally. The magenta fluorescing ChAT$^+$ cells are also found in AM lateral to the urocortin$^+$ cells, as well as dorsal and lateral to this nucleus.

Although no occurrences of overt double labeling were observed, some urocortin$^+$ cells in EW sometimes showed faint ChAT$^+$ immunolabeling. This is demonstrated in figure 7E&F. Figure 7E shows the presence of fluorescent urocortin$^+$ cells in EW and SOA when illuminated for the green fluorophore. Figure 7F shows the ChAT$^+$ cells in the same region when illuminated for the magenta fluorophore. A few highly fluorescent cells are present in EW (arrows), however some of the urocortin$^+$ cells (Fig. 7E, arrowheads) also show faint green fluorescence (Fig. 7F, arrowheads). Strassman and colleagues (1987) reported the presence of numerous cells in the cat EW that were mildly immunoreactive with ChAT antibody, with only a small population, which they felt represented the actual preganglionic motoneurons, showing intense immunoreactivity. As shown in figure 7E&F, we observed similar light staining of some of the cat EW neurons with the ChAT antibody. The fact that this effect was weak, variable and not observed in other species suggests this labeling may be spurious. Furthermore, since it appeared to correlate with background staining of other non-cholinergic neurons, we did not consider these weakly stained cells to be cholinergic, and only considered the strongly staining neurons to be ChAT$^+$ preganglionic motoneurons.

The overall distribution of the two populations, as found in immunofluorescently labeled sections like those described above (Fig. 7), is charted in figure 8. The majority of ChAT$^+$ neurons are located within the oculomotor nucleus proper and the adjacent medial longitudinal fasciculus (MLF) (Fig. 8E–J). However, ChAT$^+$ neurons are also scattered above the oculomotor nucleus in the SOA, between the two oculomotor nuclei, and ventral to the oculomotor nucleus, among its exiting fibers. Only a few intensely ChAT$^+$ cells are found within the EW. Instead, the EW is the primary location of urocortin$^+$ neurons (Fig. 8E–J). A few scattered urocortin cells are also found in the SOA and in the MRF lateral to the oculomotor nucleus. This population ends caudally at the level of the caudal central subdivision. Immediately rostral to the oculomotor nucleus (Fig. 8C&D), the urocortin$^+$ cells are primarily found in the AM. ChAT$^+$ cells are located within, dorsal and ventrolateral to the AM nucleus. Further rostrally (Fig. 8A&B), just urocortin$^+$ cells are present, which form two columns that extend into the diencephalon, on either side of the midline, ventral to the third ventricle.

DISCUSSION

Developing a Rational Nomenclature

Before considering the implications of the results of this study with respect to function, it is incumbent upon us to consider a solution for the nomenclature problem which these results present in stark form. It is now clear that the term Edinger-Westphal nucleus has been used to describe two distinct nuclei that differ dramatically in their patterns of connectivity and chemical signatures. This problem began to be evident when investigations of the location of preganglionic motoneurons in the cat showed that only a small portion of these cells were located within the cytoarchitecturally defined EW (Loewy and Saper, 1978; Loewy et al., 1978; Sugimoto et al., 1977; Toyoshima et al., 1980). This was quantified by Erichsen and May (2002), who showed that EW contains less than 5 % of the preganglionic population. The organization in the cat stands in stark contrast to that of the monkey, where the preganglionic motor neurons are largely confined to the cytoarchitecturally defined EW (Akert et al., 1980;

NIH-PA Author Manuscript

NIH-PA Author Manuscript

NIH-PA Author Manuscript

Burde and Loewy, 1980), and there is little evidence that it contains more than a minor non-preganglionic population. Similarly, the preganglionic motor neurons in the pigeon are located within the cytoarchitecturally defined EW (Reiner et al., 1983, 1991). As more species have been investigated, however, it has become evident that the location of the preganglionic motor neuron population differs appreciably from species to species, and is rarely synonymous with borders of the cytoarchitecturally defined EW (mouse: Van and Atherton, 1991; Weitemier et al., 2005; rabbit: Johnson and Purves, 1981; rat: Smeraski et al., 2004). Instead, numerous centrally projecting peptidergic populations have been found within the EW in cats, rodents and even frogs, including neurons immunoreactive for CCK, substance P, urocortin, cocaine- and amphetamine-regulated transcript (CART) and neuropeptide B (cat: Maciewicz et al., 1983; Phipps et al., 1983; present data; frog: Kozicz et al., 2002; mouse: Bachtell et al., 2002; Weitemier et al., 2005; Tanaka et al., 2003; rat: Dun et al., 2005; Hokfelt et al., 2002; Innis and Aghajanian, 1986; Kozicz et al., 1998; Kozicz, 2003). In fact, it appears that only in those species where the preganglionic motoneurons are clustered together do they occupy the cytoarchitecturally defined EW, with urocortin$^+$ cells located outside its borders (monkey: Vasconcelos et al., 2003; present data; Horn et al, submitted; pigeon: Reiner et al., 1991; Cavani et al., 2003). However, this can not even be considered a general primate or bird characteristic, since the cytoarchitecturally defined human EW has recently been shown to primarily contain urocortin$^+$ neurons (Ryabinin et al., 2005; Horn et al., submitted), and too few bird species have been sampled.

Therefore, the fact that the structures, which have been termed EW, differ in a species-specific manner with respect to their neurotransmitter content, connections and function, indicates that this term has become ambiguous as an identifier of a discrete neuronal population. It has been suggested that the terms preganglionic EW and non-preganglionic EW be used to correct this situation (Weitemeir et al., 2005; Ryabinin et al., 2005; Gaszner et al., 2007). While this clearly represents an improvement in the clarity of the terminology, this approach still does not adequately describe these sets of neurons, because the populations as a whole often ignore cytoarchitectural boundaries. For example, the diffuse distribution of preganglionic motoneurons in rodents and cats makes the term nucleus an inadequate identifier for this population. Even in monkeys, the preganglionic motoneurons extend into AM, and so are not confined to a single nucleus.

For these reasons, as well as the general trend away from the use of eponyms, we contend that the term Edinger-Westphal should be retired from active use in neuroanatomical terminology. Nonetheless, it may be useful to continue to use this term for cytoarchitecturally distinct structures in this region until suitable replacements can be agreed upon. For example, Cunha and colleagues (2007) have recently named the urocortin$^+$ population in the pigeon the subgriseal paramedian midbrain neuronal stream. For the moment, we will utilize the terms preganglionic (EW_{PG}) and urocortin-containing (EW_U) to designate these two cytoarchitecturally-defined nuclei in monkeys, and in cats and rodents (Fig. 9). However, the use of these two terms still does not solve the central dilemma caused by the fact that in many species the functional and cytoarchitectural subdivisions do not coincide; e.g., there is no distinct EW_{PG} in cats, for there is no cytoarchitecturaly defined nucleus containing preganglionic motoneurons.

To effectively deal with the complex relationships seen in these populations of neurons and the variations seen across species, we propose a new open-ended terminology, which we will employ in the rest of this report. The term perioculomotor (pIII) will be utilized as a general descriptor for all groups of neurons found in the region immediately surrounding the oculomotor nucleus (Fig. 9). This terminology was chosen because it conforms to the more descriptive nature of modern neuroanatomical terms; i.e., it tells the reader the population in question is located in the immediate vicinity of the oculomotor nucleus, without implying

NIH-PA Author Manuscript

NIH-PA Author Manuscript

NIH-PA Author Manuscript

specific function. Furthermore, it is an open-ended terminology, where individual pIII cell groups can then be designated with respect to their most relevant characteristic, invariant of their precise location. In the present case, the preganglionic parasympathetic motoneurons projecting to the ciliary ganglion will be designated the perioculomotor preganglionic population ($pIII_{PG}$). The urocortin$^+$ cells adjacent to the oculomotor nucleus will be designated the perioculomotor urocortin population ($pIII_U$). One advantage of an open ended nomenclature is that it can be applied to other groups of cells found in this region. For example, the $pIII_U$, along with the neurons that stain for other peptides may all belong to a perioculomotor peptidergic population ($pIII_P$). This designation would not work in birds, however, as preganglionic motoneurons utilize substance P and enkephalin as co-transmitters (Reiner et al., 1991). This terminology can also be employed in descriptions of other pIII cell groups. For example, those motoneurons supplying multiply innervated extraocular muscle fibers, which lie outside the oculomotor nucleus in the S and C groups (Büttner-Ennever et al., 2001;Eberhorn et al., 2005;Horn et al., submitted), may be designated as the $pIII_{S\&C}$ populations. Finally, an additional strength of this approach to the nomenclature of the pIII cell groups is that it can still be used in parallel with the extant cytoarchitectonic divisions. For example the $pIII_U$ in the monkey might be described as lying in between the oculomotor nuclei, then extending laterally in the SOA to terminate diffusely in the MRF. In summary, this new open-ended perioculomotor terminology will allow clear, precise communication among those interested in this complex region.

Oculomotor and Perioculomotor Distributions

The ChAT$^+$ population of the oculomotor complex observed here in the monkey conforms well to the population defined by the distribution of motoneurons with retrograde tracers (Buttner-Ennever and Akert, 1981; Evinger, 1988; Porter et al., 1983; Spencer and Porter, 1981). Specifically, most of these neurons were located within the cytoarchitecturally defined borders of the oculomotor nucleus and adjacent MLF, indicating they are somatic motoneurons. A group of smaller motoneurons that supply the multiply innervated muscle fibers in the extraocular muscles is found between and dorsomedial to the oculomotor nuclei proper; the S- and C-groups, respectively (Büttner-Ennever et al., 2001; Eberhorn et al., 2005; Horn et al., submitted). These $pIII_{S\&C}$ neurons were also observed in the present material (Fig. 1A&C).

The final group of ChAT$^+$ cells makes up the $pIII_{PG}$ (Fig. 9). The $pIII_{PG}$ begins in front of the caudal central subdivision, forms two clusters in the EW_{PG}, and terminates within the AM nuclei. This distribution agrees with previous descriptions of the location of the preganglionic population based on retrograde labeling from the ciliary ganglion and from ChAT immunohistochemistry (Akert et al., 1980;Burde and Loewy, 1980;Eberhorn et al., 2005;Horn-Bochtler et al., 2006;Horn et al., submitted). While the degree to which these cells were arranged into a compact group varied from section to section, we did not observe a subdivision of this population into discrete lateral, dorsal and medial visceral columns, as has been described previously (Burde, 1988;Burde and Williams, 1989).

The vast majority of ChAT$^+$ cells observed in the feline midbrain were located within the borders of the oculomotor nucleus or interspersed in the MLF (Fig. 7–9). These supply the extraocular muscles (Akagi, 1978;Gacek, 1974;Spencer and Porter, 1981). Only a few ChAT$^+$ pIII cells were found within the cat EW_U. Instead, numerous labeled cells were scattered in the supraoculomotor area, ventrolateral to the MLF, and within and ventrolateral to AM (Fig. 8). This general pattern of pIII ChAT$^+$ cells closely matches that of the cells retrogradely labeled from the ciliary ganglion (Erichsen and May, 2002;Loewy and Saper, 1978;Loewy et al., 1978;Sugimoto et al., 1977;Toyoshoma et al., 1980), and trans-neuronally from the eye (Erichsen and May, 2002). The overall distribution of ChAT$^+$ labeling is much the same as that reported by Strassman and colleagues (1987).

NIH-PA Author Manuscript

NIH-PA Author Manuscript

NIH-PA Author Manuscript

In the macaque, the $pIII_U$ population was mainly located in a fountain-shaped group that began between the two oculomotor nuclei and extended dorsolaterally into the supraoculomotor area, with scattered cells in the MRF and InC (fig. 9). Rostrally, the $pIII_U$ population extended into the AM nucleus, but was not restricted by its borders (Fig. 2). This distribution was also observed in old world monkeys by Horn and colleagues (submitted), and appears to be generally similar to that seen in the new world monkey, *Cebus paella* (Vasconcelos et al., 2003), based on immunohistochemistry and *in situ* hybridization. This pattern is similar in many respects to that observed for rat urocortin$^+$ cells (Bittencourt et al., 1999).

In the cat, the main $pIII_U$ population is found in EW_U (Fig. 6&9). Only scattered cells are found in the cat SOA and the MRF, lateral to the oculomotor nucleus. The fact the cat $pIII_U$ does not have to avoid a consolidated $pIII_{PG}$, like that found in the monkey, may partially explain its different organization. Rostrally, the $pIII_U$ extends through the AM, as in the monkey, but then extends even further rostrally as two discrete columns. The reason for these species differences merits study. The distribution of the $pIII_U$ population also overlaps extensively with that of other peptides in the cat (Maciewicz et al., 1983; and Phipps et al., 1983) including substance P and CCK, suggesting the $pIII_U$ population is part of a larger pIII peptidergic population ($pIII_P$). The degree of coexpression of these peptides is just beginning to be explored. In the rat, urocortin has been found to be co-expressed with CCK, but not substance P (Gysling et al., 2006).

Separate Perioculomotor Populations

The results of the present study clearly indicate that the urocortin$^+$ cells and the ChAT$^+$ cells found in the midbrain of both the cat and monkey represent two separate populations. This conclusion is supported by the results of the immunofluorescence experiments shown here in figures 3 and 7 (also Horn et al., submitted). No cells were seen that exhibited strong fluorescence with both fluorophores, which would have been indicated by a yellow color when the digitized images were combined. These findings correspond to those of Weitemier and colleagues (2005) in the mouse, where no overlap between these two immunohistochemically defined populations was found. Similarly, immunohistochemical staining for urocortin and ChAT in the same sections in new world monkeys (*Cebus appella*) also showed that these two populations, while distributed adjacent to one another, are separate (Vasconcelos et al., 2003). Finally, immunohistochemical examination of autopsy material reveals that this same dichotomy is present in the human midbrain (Ryabinin et al., 2005; Horn et al., submitted). Assuming the fact that both somatic and preganglionic motoneurons are cholinergic, and hence likely to be ChAT$^+$, the evidence presented here, and the studies cited above, strongly indicate that the outflow of the oculomotor nerve is not urocortin$^+$ in mammalian species.

While the $pIII_{PG}$ population appears to be made up of ChAT$^+$ motoneurons, it seems likely that $pIII_U$ cells found in the midbrain project to targets within the neuraxis (Fig. 9). Urocortin$^+$ terminals are distributed widely in the brain, although they are relatively rare within the telencephalon (mouse: Weitemeir et al., 2005; monkey: Vasconcelos et al., 2003; rat: Bittencourt et al., 1999). As the only other regions reported to contain significant numbers of highly urocortin$^+$ cells are the lateral superior olive and supraoptic nucleus (Bittencourt et al., 1999;Weitemeir et al., 2005;Vasconcelos et al., 2003), it seems reasonable to conclude that the $pIII_U$ population may provide widespread central projections.

Functional Implications

With little over a decade of study (Vaughan et al., 1995), our understanding of the actions of the neuropeptide, urocortin, is still limited. Central urocortin administration appears to have distinct behavioral effects: producing stress-related behaviors, and decreasing appetite for food, water and even sexual activity (Heinrichs and Richard, 1999; Spina et al., 1996). Still,

NIH-PA Author Manuscript

NIH-PA Author Manuscript

NIH-PA Author Manuscript

we can not know from drug administration studies whether these responses indicate the action of actual urocortin circuits. Nevertheless, there is strong evidence for urocotin's role in these functions. Specifically, correlative experiments show that manipulations related to stress and diet appear to produce changes in urocortin or c-fos expression in EW_U (Bachtell et al., 1999; 2002; Gaszner et al., 2004; Kozicz et al., 2001; Weitemier et al., 2001), and lesion experiments indicate that loss of the area containing the $pIII_U$ population produces changes in food and water consumption (Weitemier and Ryabinin, 2005). The latter study showed no changes in basal metabolic rate or exploratory activity, suggesting that the role of EW_U may not be as important for stress responses. These findings reinforce other studies that show activity changes in this region mirror a predisposition to alcohol consumption, but do not affect pupillary constriction, as would be expected for the $pIII_{PG}$ (Bachtell et al., 2002; 2003).

In order to further dissect the function of the $pIII_U$ population, we need to better define the projections of this group (Fig. 9). Retrograde tracing studies in the rat have shown that the $pIII_U$ population sends projections to the spinal cord and the lateral septal nucleus (Bittencourt et al., 1999). In addition, electrolytic lesions of the $pIII_U$ lead to a significant decrease in the number of urocortin$^+$ fibers in the lateral septum and dorsal raphe in the mouse (Bachtell et al., 2003). Studies of the latter projection indicate a role in energy expenditure (Turek and Ryabinin; 2005;Weitemier and Ryabinin, 2006). Studies of projections to the lateral septum suggest involvement in appetite, in particular for alcohol (Bachtell et al., 2003;Ryabinin and Weitemier, 2006). The functions of descending pathways to the spinal cord have not been defined, although a role in sympathetic control has been proposed based on the large number of urocortin$^+$ fibers observed in the intermediolateral cell column (Bittencourt, 1999). This is in line with other studies showing projections from the various pIII peptidergic populations to the spinal cord (cat: Chung et al., 1987;Loewy et al., 1978;Maciewicz et al., 1983;Phipps et al., 1983;Sugimoto et al., 1978; monkey: Burde, 1988). Finally, cerebellar injections have been shown to label neurons whose distribution overlaps that of the $pIII_U$ population in the cat (Sugimoto et al., 1978;Røste and Dietrichs, 1988a&b) and the monkey (May et al., 1992).

The functional implications of the location of this urocortin population, and the related peptidergic neurons, as a pIII group are unclear. It may be that their position rostral to the dorsal raphe is more telling, and their relationship to the oculomotor nucleus is just a developmental or evolutionary happenstance. Certainly, their pattern of projection, and use of specialized neurotransmitters is reminiscent of the more caudally distributed serotonergic dorsal raphe, although these are geographically separate populations. Nevertheless, while we have shown here that the $pIII_U$ and $pIII_{PG}$ populations clearly have distinctly different distribution patterns, there is also no question but that they have some overlap in their somatic distribution, and considerable overlap in their dendritic fields. Furthermore, it would appear that the distribution of the $pIII_U$ population is likely to overlap with that of C- and S-group motoneurons that supply non-twitch muscle fibers in the extraocular muscles in the monkey (Büttner-Ennever et al., 2001; Eberhorn et al., 2005), and perhaps in the rat (Eberhorn et al., 2006). Certainly, it would appear that the dendrites of these motoneurons would pass through the $pIII_U$ population (May et al., 2000). Consequently, the possibility that these populations have some level of common input, and perhaps even a degree of common function, must be entertained. In this regard, it should be noted that there is an extensive urocortin$^+$ terminal distribution in the vestibular nuclei (Monkey: Vasconcelos et al., 2003; mouse: Weitemier et al., 2005; rat: Bittencourt et al., 1999). Thus, the possibility that these distinct pIII populations share some inputs and aspects of function remains an open and testable hypothesis.

Acknowledgments

Supported by: NIH Grant # EY014263 (PJM), EY-05928 (AJR) and #AA013738 (AER)

NIH-PA Author Manuscript

NIH-PA Author Manuscript

NIH-PA Author Manuscript

We would like to thank Olga Golanov, Sherry Cuthbertson, Raven Blalock and Ronjon Datta for their assistance with the immunohistochemical work done in this study.

LIST OF ABBREVIATIONS

AM	anteromedian nucleus
CART	cocaine- and amphetamine-regulated transcript
CC	caudal central subdivision
CCK	cholecystokinin
ChAT	choline acetyl transferase
EW	Edinger-Westphal nucleus
EW_{PG}	preganglionic EW
EW_{U}	urocortin containing EW
III	oculomotor nucleus
IIIn	oculomotor nerve rootlets
InC	interstitial nucleus of Cajal
MLF	medial longitudinal fasciculus
MRF	midbrain reticular formation
nD	nucleus Darkschewitsch
PAG	periaqueductal gray
PC	posterior commissure
pIII	perioculomotor region
$pIII_{P}$	perioculomotor peptidergic population
$pIII_{PG}$	perioculomotor preganglionic motoneurons
$pIII_{S\&C}$	periculomotor S- and C-group motoneurons
$pIII_{U}$	perioculomotor urcortin^{+} neurons
PVG	periventricular gray
RF	fasciculus retroflexus
SOA	supraoculomotor area

LITERATURE CITED

Adams JC. Heavy metal intensification of DAB-based HRP reaction product. J Histochem Cytochem 1981;29:775. [PubMed: 7252134]

Akagi Y. The localization of the motor neurons innervating the extraocular muscles in the oculomotor nuclei of cat and rabbit, using horseradish peroxidase. J Comp Neurol 1978;181:745–762. [PubMed: 690283]

Akert K, Glicksman MA, Lang W, Grob P, Huber A. The Edinger-Westphal nucleus in the monkey. A retrograde tracer study. Brain Res 1980;184:491–498. [PubMed: 6153290]

Bachtell RK, Wang Y-M, Freeman P, Risinger FO, Ryabinin AE. Alcohol drinking produces region-selective changes in expression of inducible transcription factors. Brain Res 1999;847:157–165. [PubMed: 10575084]

NIH-PA Author Manuscript

NIH-PA Author Manuscript

NIH-PA Author Manuscript

Bachtell RK, Tsivkovskaia NO, Ryabinin AE. Alcohol-induced c-Fos expression in the Edinger-Westphal nucleus: Pharmacological and signal transduction mechanisms. J Pharmacol Exp Ther 2002;302:516–524. [PubMed: 12130710]

Bachtell RK, Weitemier AZ, Galvan-Rosas A, Tsivkovskaia NO, Risinger FO, Phillips TJ, Grahame NJ, Ryabinin AE. The Edinger-Westphal-lateral septum urocortin pathway and its relationship to alcohol consumption. J Neurosci 2003;23:2477–2487. [PubMed: 12657708]

Bale TL, Vale WW. CRF and CRF receptors: role in stress responsivity and other behaviors. Annu Rev Pharmacol Toxicol 2004;44:525–557. [PubMed: 14744257]

Bittencourt JC, Vaughan J, Arias C, Rissman RA, Vale WW, Sawchenko PE. Urocortin expression in rat brain: Evidence against a pervasive relationship of urocortin-containing projections with targets bearing type 2 receptors. J Comp Neurol 1999;415:285–312. [PubMed: 10553117]

Burde RM, Loewy AD. Central origin of oculomotor parasympathetic neurons in the monkey. Brain Res 1980;198:434–439. [PubMed: 7407608]

Burde RM. Disparate visceral neuronal pools subserve spinal cord and ciliary ganglion in the monkey: a double labeling approach. Brain Res 1988;440:177–180. [PubMed: 2451977]

Burde RM, Williams F. Parasympathetic nuclei. Brain Res 1989;498:371–375. [PubMed: 2790489]

Büttner-Ennever JA, Akert K. Medial rectus subgroups of the oculomotor nucleus and their abducens internuclear input in the monkey. J Comp Neurol 1981;197:17–27. [PubMed: 6894456]

Büttner-Ennever JA, Horn AKE, Scherberger H, D'Ascanio P. Motoneurons of twitch and nontwitch extraocular muscle fibers in the abducens, trochlear, and oculomotor nuclei of monkeys. J Comp Neurol 2001;438:318–335. [PubMed: 11550175]

Cavani JA, Reiner A, Cuthberson SL, Bittencourt JC, Toledo CAB. Evidence that urocortin is absent from neurons of the Edinger-Westphal nucleus in pigeons. Brazilian J Med Biol Res 2003;36:1700.

Chung RY, Mason P, Strassman A, Maciewics RJ. Edinger-Westphal nucleus: cells that project to spinal cord contain corticotropin-releasing factor. Neurosci Lett 1987;83:13–19. [PubMed: 2831475]

Clarke RJ, Coimbra CJP, Alessio ML. Distribution of parasympathetic motoneurons in the oculomotor complex innervating the ciliary ganglion in the marmoset (*Callithrix jacchus*). Acta Anat 1985;121:53–58. [PubMed: 3918402]

Crawford K, Terasawa E, Kaufman PL. Reproducible stimulation of ciliary muscle contraction in cynomologous monkey via a permanent indwelling midbrain electrode. Brain Res 1989;503:265–272. [PubMed: 2605519]

Cunha RP, Reiner A, Toledo CAB. Involvement of urocortinergic neurons below the midbrain central gray in the physiological response to restraint stress in pigeons. Brain Res. 2007 (EPub).

Dun SL, Brailoiu, Mizuo K, Yang J, Chang JK, Dun NJ. Neuropeptide B immunoreactivity in the central nervous system of the rat. Brain Res 2005;1045:157–163. [PubMed: 15910774]

Eberhorn AC, Ardeleanu P, Büttner-Ennever JA, Horn AKE. Histochemical differences between motoneurons supplying multiply and singly innervated extraocular muscle fibers. J Comp Neurol 2005;491:352–366. [PubMed: 16175553]

Eberhorn AC, Büttner-Ennever JA, Horn AKE. Identification of motioneurons supplying multiply- or singly-innervated extraocular muscle fibers in the rat. Neurosci 2006;137:891–903.

Edinger L. Über den Verlauf der centralen Hirnnervenbahnen mit Demonstrationen von Präparaten. Arch Psychiat Nervenerkr 1885;16:858–859.

Erichsen JT, May PJ. The pupillary and ciliary components of the cat Edinger-Westphal nucleus: A transsynaptic transport investigation. Visual Neurosci 2002;19:15–29.

Evinger, C. Extraocular motor nuclei: location, morphology and afferents. In: Büttner-Ennever, JA., editor. Neuroanatomy of the Oculomotor System. Amsterdam: Elsevier; 1988. p. 81-117.

Fekete EV, Zorrilla EP. Physiology, pharmacology, and therapeutic relevance of urocortins in mammals: Ancient CRF paralogs. Front Neuroendocrinol. 2006 (EPub).

Fitzgerald MEC, Vana B, Reiner A. Control of choroidal blood flow by the nucleus of Edinger-Westphal: A laser-Doppler study. Invest Ophthalmol Vis Sci 1990;31:2483–2492. [PubMed: 2265988]

Fitzgerald MEC, Gamlin PDR, Zagvazdin Y, Reiner A. Central neural circuits for the light-mediated reflexive control of choroidal blood flow in the pigeon eye: A laser Doppler study. Visual Neurosci 1996;13:655–669.

NIH-PA Author Manuscript

NIH-PA Author Manuscript

NIH-PA Author Manuscript

Gacek RR. Localization of neurons supplying the extraocular muscles in the kitten using horseradish peroxidase. Exp Neurol 1974;44:381–403. [PubMed: 4621069]

Gamlin PDR, Reiner A. The Edinger-Westphal nucleus: Sources of input influencing accommodation, pupilloconstriction, and choroidal blood flow. J Comp Neurol 1991;306:425–438. [PubMed: 1713924]

Gamlin PDR, Zhang Y, Clendaniel RA, Mays LE. Behavior of identified Edinger-Westphal neurons during ocular accommodation. J Neurophysiol 1994;72:2368–2382. [PubMed: 7884465]

Gaszner B, Csernus V, Kozicz T. Urocortinergic neurons respond in a differentiated manner to various acute stressors in the Edinger-Westphal nucleus in the rat. J Comp Neurol 2004;480:170–179. [PubMed: 15514930]

Gaszner B, Korosi A, Palkovits M, Roubos EW, Kozicz T. Neuropeptide Y activates urocortin 1 neurons in the nonpreganglionic Edinger-Westphal nucleus. J Comp Neurol 2007;500:708–719. [PubMed: 17154253]

Gysling K, Blanco EH, Quiroz G. Neuroanatomical studies on the non-preganglionic Edinger-Westphal nucleus of the rat: Substance P and CART peptides are expressed in distinct neurons. Soc Neurosci Abst #6887. 2006

Hauger RL, Grigoriadis DE, Dallman MF, Plotsky PM, Vale WW, Dautzenberg FM. International Union of Pharmacology. XXXVI. Current status of the nomenclature for receptors for corticotropin-releasing factor and their ligands. Pharm Rev 2003;55:21–26. [PubMed: 12615952]

Heinrichs SC, Richard D. The role of corticotropin-releasing factor and urocortin in the modulation of ingestive behavior. Neuropeptides 1999;33:350–359. [PubMed: 10657512]

Hokfelt T, Blacker D, Broberger C, Herrera-Marschitz M, Snyder G, Fisone G, Cortes R, Morino P, You Z-B, Ogren SO. Some aspects of the anatomy and function of central cholecystokinin systems. Parmacol Toxicol 2002;91:383–386.

Horn AK, Eberhorn A, Härtig W, Ardeleanu A, Büttner-Ennever JA. Preoculomotor cell groups in monkey an man defined by their histochemical and functional properties: A reappraisal of the Edinger-Westphal nucleus. J Comp Neurol. Submitted.

Horn-Bochtler AK, Ardeleanu P, Messoudi A, Büttner-Ennever JA. Histochemical characteristics of cell groups in the perioculomotor area, including the Edinger-Westphal complex, in monkey and man. Soc Neurosci Abst #2459. 2006

Innis RB, Aghajanian GK. Cholecystokinin-containing and nociceptive neurons in rat Edinger-Westphal nucleus. Brain Res 1986;363:230–238. [PubMed: 3942895]

Johnson DA, Purves D. Post-natal reduction of neural unit size in the rabbit ciliary ganglion. J Physiol (Lond) 1981;318:143–159. [PubMed: 7320886]

Kozicz T, Yanaihara H, Arimura A. Distribution of urocortin-like immunoreactivity in the central nervous system of the rat. J Comp Neurol 1998;391:1–10. [PubMed: 9527535]

Kozicz T, Li M, Arimura A. The activation of urocortin immunoreactive neurons in the Edinger-Westphal nucleus following acute pain stress in rats. Stress 2001;4:85–90.

Kozicz T, Arimura A, Maderdrut JL, Lazar G. Distribution of Urocortin-like immunoreactivity in the central nervous system of the frog Rana esculenta. J Comp Neurol 2002;453:185–198. [PubMed: 12373783]

Kozicz T. Neurons colocalizing urocortin and cocaine and amphetamine-regulated transcript immunoreactivities are induced by acute lipopolysaccharide stress in the Edinger-Westphal nucleus in the rat. Neurosci 2003;116:315–320.

Kozicz T, Korosi A, Korsman C, Tilburg-Ouwens D, Groenink L, Veening J, Van der Gugten J, Roubos E, Olivier B. Urocortin expression in the Edinger-Westphal nucleus is down-regulated in transgenic mice over-expressing neuronal corticotropin-releasing factor. Neurosci 2004;123:589–594.

Leger J, Croll RP, Smith FM. Regional distribution and extrinsic innervation of intrinsic cardiac neurons in the guinea pig. J Comp Neurol 1999;407:303–317. [PubMed: 10320213]

Lim MM, Tsivkovskaia NO, Bay Y, Young LJ, Ryabinin AE. Distribution of corticotropin-releasing factor and urocortin 1 in the vole brain. Brain Behav Evol 2006;68:229–240. [PubMed: 16816534]

Loewy AD, Saper SB. Edinger-Westphal nucleus: projections to the brainstem and spinal cord in the cat. Brain Res 1978;150:1–27. [PubMed: 78743]

NIH-PA Author Manuscript

NIH-PA Author Manuscript

NIH-PA Author Manuscript

Loewy AD, Saper CB, Yamodis D. Re-evaluation of the efferent projections of the Edinger-Westphal nucleus in the cat. Brain Res 1978;141:153–159. [PubMed: 624070]

Maciewicz R, Phipps BS, Foote WE, Aronin N, DiFiglia M. The distribution of substance P-containing neurons in the cat Edinger-Westphal nucleus: relationship to efferent projection systems. Brain Res 1983;270:217–230. [PubMed: 6192874]

Maciewicz R, Phipps BS, Grenier J, Poletti CE. Edinger-westphal nucleus: cholecystokinin immunocytochemistry and projections to spinal cord and trigeminal nucleus in the cat. Brain Res 1984;299:139–145. [PubMed: 6202372]

May PJ, Porter JD, Gamlin PDR. Interconnections between the primate cerebellum and midbrain near-response regions. J Comp Neurol 1992;315:98–116. [PubMed: 1371782]

May PJ, Wright R, Lin C-S, Erichsen JT. Light and electron microscopic features of medial rectus C-subgroup motoneurons in macaques suggest near triad specialization. Invest Ophthalmol Vis Sci 2000;41:S820.

Morin SM, Ling N, Liu X-L, Kahl SD, Gehlert DR. Differential distribution of urocortin- and corticotropin-releasing factor in the rat brain. Neurosci 1999;92:281–291.

Olszewski, J.; Baxter, D. Cytoarchitecture of the human brain stem. Basel, München, Paris, London, New York, Sydney: S. Krager; 1982.

Paxinos, G.; Watson, C. The Rat Brain in Stereotaxic Coordinates. San Francisco: Academic press; 1982.

Paxinos, G.; Franklin, K. The Mouse Brain Atla in Stereotaxic Coordinates. San Diego: Academic Press; 2001.

Phipps BS, Maciewicz R, Sandrew BB, Poletti CE, Foote WE. Edinger-Westphal neurons that project to spinal cord contain substance P. Neurosci Lett 1983;36:125–131. [PubMed: 6191256]

Porter JD, Guthrie BL, Sparks DL. Innervation of monkey extraocular muscles: Localization of sensory and motor neurons by retrograde transport of horseradish peroxidase. J Comp Neurol 1983;218:208–219. [PubMed: 6604075]

Reiner A, Karten HJ, Gamlin PDR, Erichsen JT. Parasympathetic ocular control. Functional subdivisions and circuitry of the avian nucleus of Edinger-Westphal. Trends Neurosci 1983;6:140–145.

Reiner A, Erichsen JT, Cabot JB, Evinger C, Fitzgerald MEC, Karten HJ. Neurotransmitter organization of the nucleus of Edinger-Westphal and its projection to the avian ciliary ganglion. Visual Neurosci 1991;6:451–472.

Røste GK, Dietrichs E. Cerebellar cortical and nuclear afferents from the Edinger-Westphal nucleus in the cat. Anat Embryol 1988a;178:59–65.

Røste GK, Dietrichs E. The feline oculomotor nucleus: morphological subdivisions and projection to the cerebellar cortex and nuclei. Anat Embryol 1988b;178:67–75.

Ryabinin AE, Tsivkovskaia NO, Ryabinin SA. Urocortin 1-containing neurons in the human Edinger-Westphal nucleus. Neurosci 2005;134:1317–1323.

Ryabinin AE, Weitemier AZ. The urocortin1 neurocircuit: Ethanol sensitivity and potential involvement in alcohol consumption. Brain Res Rev 2006;52:368–380. [PubMed: 16766036]

Skelton KH, Owens MJ, Nemeroff CB. The neurobiology of urocortin. Regul Peptides 2000;93:85–92.

Smeraski CA, Sollars PJ, Ogilvie MD, Enquist LW, Pickard GE. Suprachiasmatic nucleus input to autonomic circuits identified by retrograde transsynaptic transport of pseudorabies virus from the eye. J Comp Neurol 2004;471:298–313. [PubMed: 14991563]

Spencer RF, Porter JD. Innervation and structure of extraocular muscles in the monkey in comparison to those of the cat. J Comp Neurol 1981;198:649–665. [PubMed: 7251934]

Spina M, Merlo-Pich E, Chan RKW, Basso AM, Rivier J, Vale W, Koob GF. Appetite-suppressing effects of urocortin, a CRF-related neuropeptide. Science 1996:1561–1564. [PubMed: 8703220]

Strassman A, Mason P, Eckenstein FP, Baughman RW, Maciewics RJ. Choline acetyltransferase immunocytochemistry of Edinger-Westphal and ciliary ganglion afferent neurons in the cat. Brain Res 1987;423:293–304. [PubMed: 2445447]

Sugimoto T, Itoh K, Mizuno N. Localization of neurons giving rise to the oculomotor parasympathetic outflow: a HRP study in cat. Neurosci Lett 1977;7:301–305. [PubMed: 19605130]

Sugimoto T, Itoh K, Mizuno N. Direct projections from the Edinger-Westphal nucleus to the cerebellum and spinal cord in the cat: an HRP study. Neurosci Lett 1978;9:17–22. [PubMed: 19605187]

NIH-PA Author Manuscript

NIH-PA Author Manuscript

NIH-PA Author Manuscript

Sun W, May PJ. Organization of the extraocular and preganglionic motoneurons supplying the orbit in the lesser Galago. Anat Rec 1993;237:89–103. [PubMed: 7692768]

Tanaka H, Yoshida T, Miyamoto N, Motoike T, Kurosu H, Shibata K, Yamanaka A, Williams SC, Richardson JA, Tsujino N, Garry MG, Lerner MR, King DS, O'Dowd BF, Sakurai T, Yanagisawa M. Characterization of a family of endogenous peptide ligands for the G protein-coupled receptors GPR7 and GPR8. Proc Natl Acad Sci USA 2003;100:6251–6256. [PubMed: 12719537]

Toyoshima K, Kawana E, Sakai H. On the neuronal origin of the afferents to the ciliary ganglion in cat. Brain Res 1980;185:67–76. [PubMed: 7353181]

Turek VF, Ryabinin AE. Ethanol versus lipopolysaccharide-induced hypothermia: involvement of urocortin. Neurosci 2005;133:1021–1028.

Vale W, Spiess J, Rivier C, Rivier J. Characterization of a 41-residue ovine hypothalamic peptide that stimulates secretion of corticotropin and beta-endorphin. Science 1981;213:1394–1397. [PubMed: 6267699]

Vann VR, Atherton SS. Neural spread of herpes simplex virus after anterior chamber inoculation. Invest Ophthalmol Vis Sci 1991;32:2462–2472. [PubMed: 1714427]

Vasconcelos LAP, Donaldson C, Sita LV, Casatti CA, Lotfi CFP, Wang LQ, Cadinouche MZA, Frigo L, Elias CF, Lovejoy DA, Bittencourt JC. Urocortin in the central nervous system of a primate (*Cebus apella*): Sequencing, immunohistochemical, and hybridization histochemical characterization. J Comp Neurol 2003;463:157–175. [PubMed: 12815753]

Vaughan J, Donaldson C, Bittencourt JC, Perrin MH, Lewis K, Sutton S, Chan R, Turnbull AW, Lovejoy D, Rivier C, Rivier J, Sawchenko PE, Vale W. Urocortin, a mammalian neuropeptide related to fish urotensin I and to corticotropin-releasing factor. Nature 1995;378:287–292. [PubMed: 7477349]

Vilupuru AS, Glasser A. The relationship between refractive and biometric changes during Edinger-Westphal stimulated accommodation in rhesus monkeys. Exp Eye Res 2005;80:349–360. [PubMed: 15721617]

Weitemier AZ, Woerner A, Backstro mP, Hyytia P, Ryabinin AE. Expression of c-Fos in alko alcohol rats responding for ethanol in an operant paradigm. Alcohol Clin Exp Res 2001;25:704–710. [PubMed: 11371719]

Weitemier AZ, Ryabinin AE. Lesions of the Edinger-Westphal nucleus alter food and water consumption. Behav Neurosci 2005;119:1235–1243. [PubMed: 16300431]

Weitemier AZ, Ryabinin AE. Urocortin 1 regulates food and fluid consumption, but not ethanol preference in C57BL/6J mice. Neurosci 2006;137:1439–1445.

Weitemier AZ, Tsivkovskaia NO, Ryabinin AE. Urocortin 1 distribution in mouse brain is strain-dependent. Neurosci 2005;132:729–740.

Weninger SC, Peters LL, Majzoub JA. Urocortin expression in the Edinger-Westphal nucleus is up-regulated by stress and corticotropin-releasing hormone deficiency. Endocrinology 2000;141:256–263. [PubMed: 10614646]

Westphal C. Über einen Fall von chronischer progressiver Lähmung der Augenmuskeln (Ophtalmopregia externa) nebst Beschreibung von Ganglienzellengruppen im Bereiche des Oculomotoriuskerns. Arch Psychiat Nervenheilk 1887;98:846–871.

Yamamoto H, Maeda T, Fujimura M, Fujimiya M. Urocortin-like immunoreactivity in the substantia nigra, ventral tegmental area and Edinger-Westphal nucleus of rat. Neurosci Lett 1998;243:21–24. [PubMed: 9535103]

NIH-PA Author Manuscript
NIH-PA Author Manuscript
NIH-PA Author Manuscript

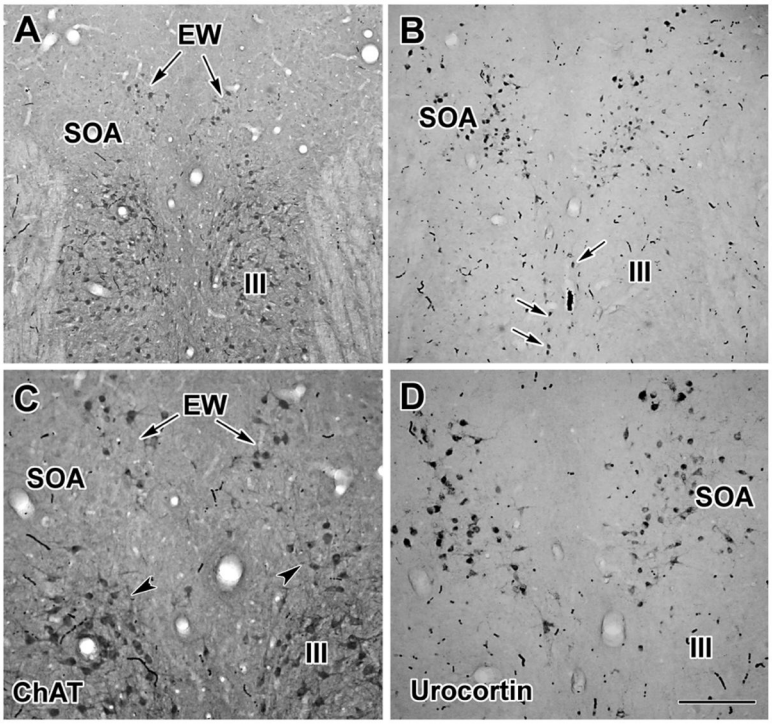

Figure 1.

Low (A&B) and high (C&D) magnification views of the labeling of neurons in and around the monkey oculomotor nucleus (III) and Edinger-Westphal nucleus (EW) with antibodies to ChAT (A&C) and urocortin (B&D). Arrows in B indicate urocortin^{+} neurons in between the oculomotor nuclei. Arrowheads in C indicate C&S-group motoneurons. Scale bar = 500:m in A&B and 250:m in C&D.

NIH-PA Author Manuscript

NIH-PA Author Manuscript

NIH-PA Author Manuscript

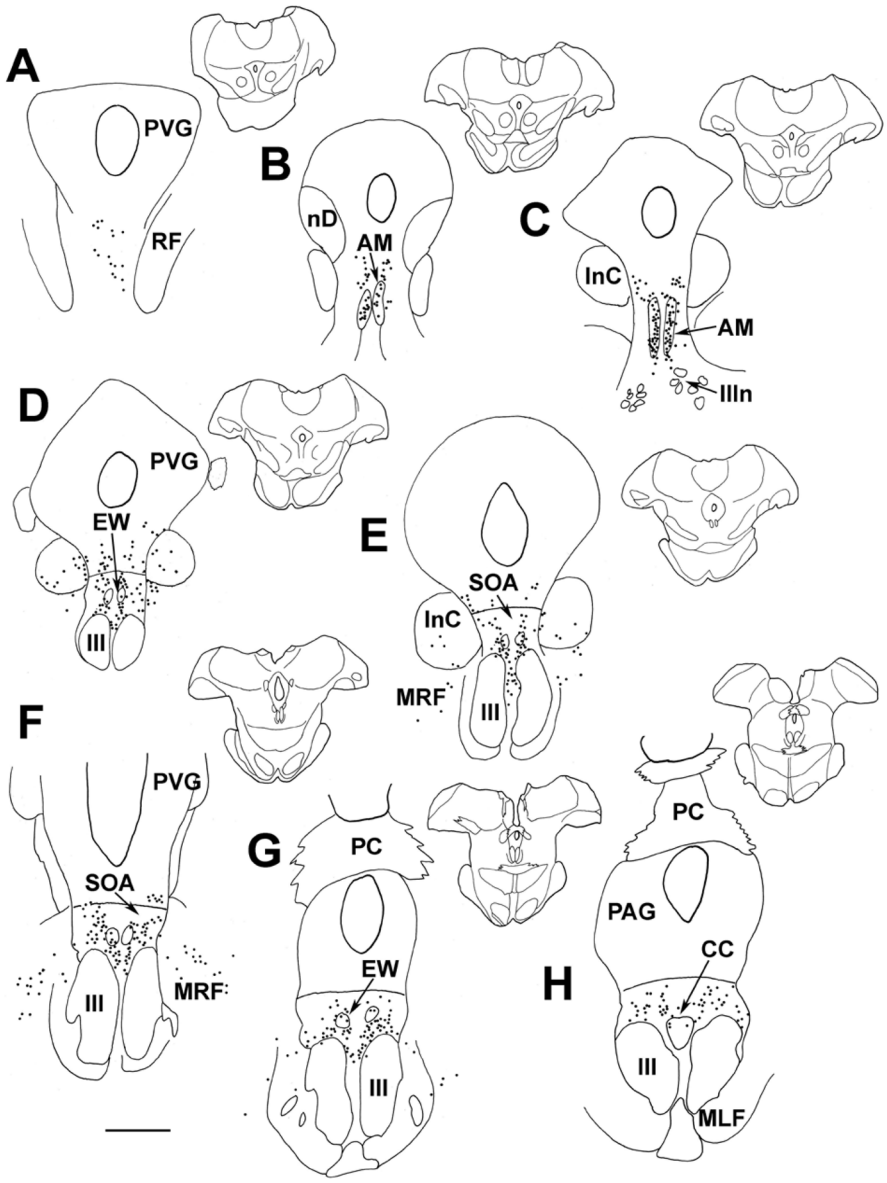

Figure 2.

Rostral (A) to caudal (H) charting of the distribution of urocortin^{+} neurons in the monkey perioculomotor region. Numerous urocortin^{+} cells are found within the anteromedian nucleus (AM), as well as dorsal and rostral to it (A–C). Large numbers of urocortin^{+} cells are also found in the supraoculomotor area (SOA) (D–H), but extend dorsal to this region onto the periventricular gray (PVG) and laterally into the interstitial nucleus of Cajal (InC) (D&E) and midbrain reticular formation (MRF) (E–G). This population does not extend past the caudal central subdivision (H). Scale bar = 1.0 mm.

NIH-PA Author Manuscript
NIH-PA Author Manuscript
NIH-PA Author Manuscript

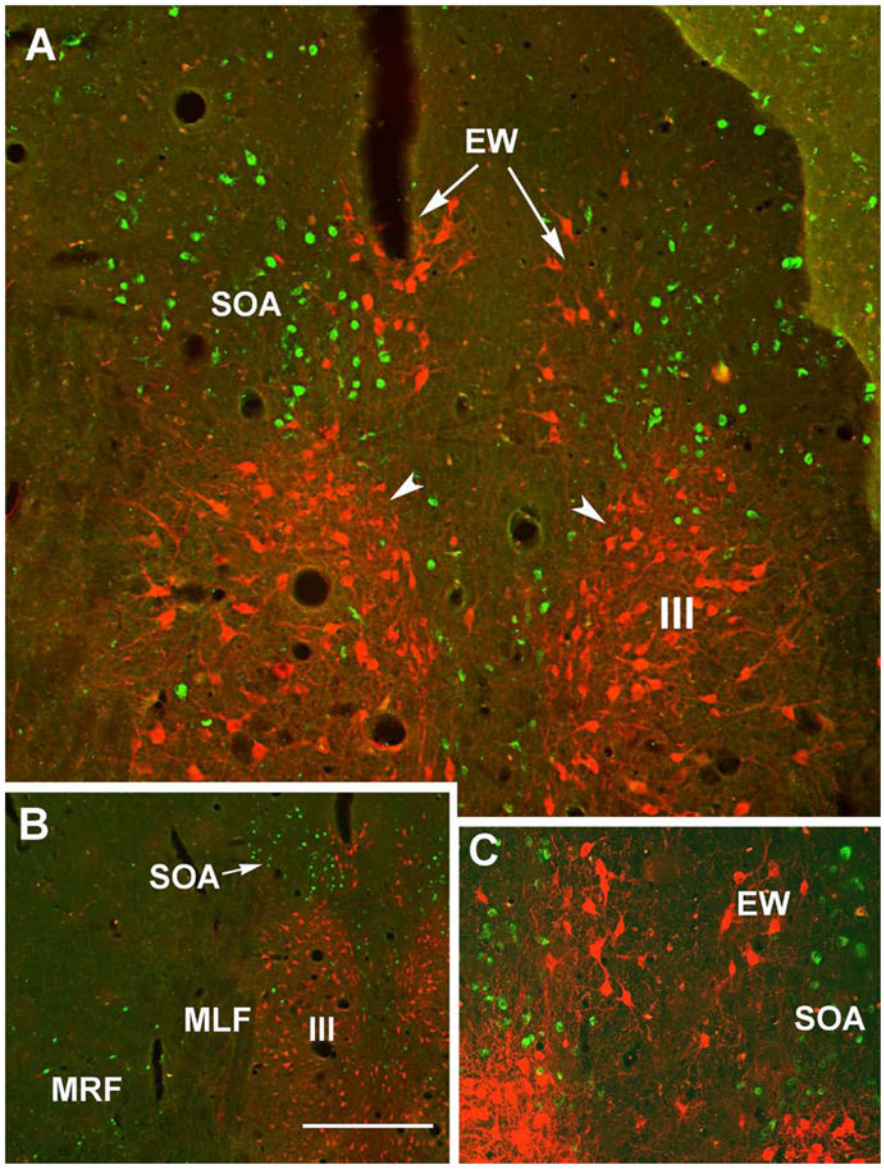

Figure 3.

Combined immunofluorescent images to simultaneously demonstrate urocortin^{+} (green) and ChAT^{+} (magenta) neurons in the monkey. Plate A shows a high magnification view of the section shown in B from the middle of the oculomotor nucleus (III), while C is from the rostral end of the oculomotor nucleus. ChAT^{+} cells are found within the oculomotor nucleus and in paired columns dorsal to the oculomotor nucleus, making up the Edinger-Westphal nucleus (EW). Small magenta cells along the dorsomedial edge of the oculomotor nucleus (arrowheads) represent C&S-group motoneurons. There is overlap between their distribution and that of the urocortin^{+} cells (A&C). The main body of urocortin^{+} cells has a fountain-shaped distribution in A&B, beginning medially, between the oculomotor nuclei and extending laterally in the supraoculomotor area (SOA). Note that in B, urocortin^{+} cells are also present in the midbrain reticular formation (MRF) and a few cells are located within the oculomotor nucleus in A. [N.B. red has been digitally altered to magenta at the request of the journal.] Scale bar = 1.0 mm for B, o.5 mm for A&C.

NIH-PA Author Manuscript
NIH-PA Author Manuscript
NIH-PA Author Manuscript

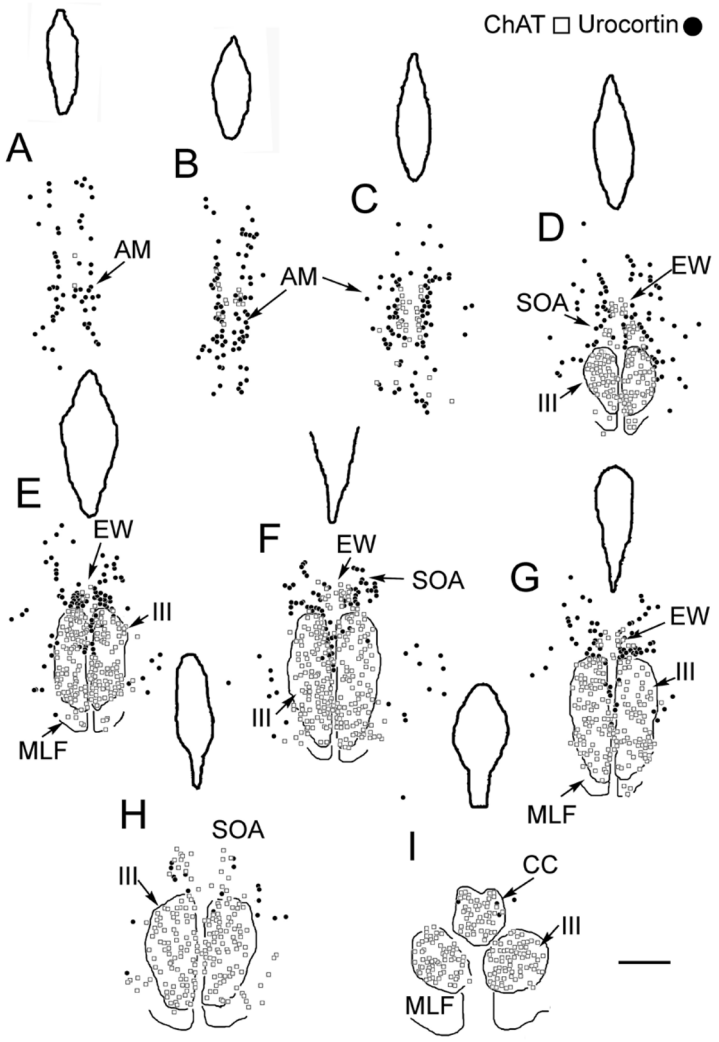

Figure 4.

Charting of the distributions of ChAT$^+$ (Q) and urocortin$^+$ (M) neurons in the monkey from sequential fluorescence immunohistochemistry sections like those illustrated in figure 3. AI is a rostral to caudal series. ChAT$^+$ neurons have a more medial, and dorsoventrally constrained distribution in the anteromedian nucleus (AM) than the urocortin$^+$ cells, which also extend dorsal to AM (A–C). At more caudal levels (E–H), urocortin$^+$ cells are primarily found medial to the oculomotor nucleus and dorsal to it in the supraoculomotor area (SOA). Urocortin$^+$ neurons are also found laterally in the midbrain reticular formation (MRF). Most of the ChAT$^+$ cells are found within the oculomotor nucleus (III) or grouped within the Edinger-Westphal nucleus (EW). The urocortin$^+$ distribution ends caudally (I), at the level of the caudal central subdivision (CC). Scale bar = 1.0 mm.

NIH-PA Author Manuscript

NIH-PA Author Manuscript

NIH-PA Author Manuscript

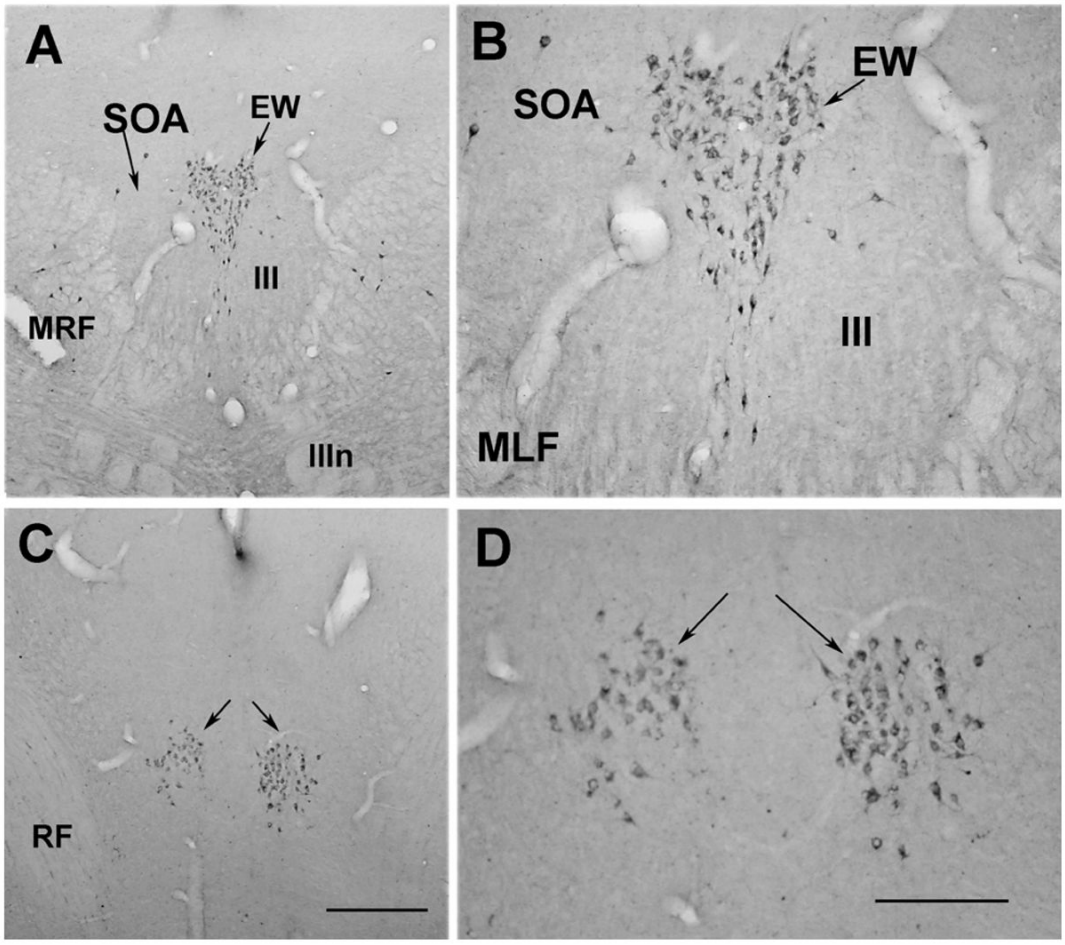

Figure 5.

Low (A&C) and high (B&D) magnification views of the labeling of neurons in and around the cat oculomotor nucleus (III) with antibodies to urocortin. In A&B, a section through the middle of the oculomotor nucleus, most of the urocortin positive cells are found within the midline Edinger-Westphal nucleus (EW). However, scattered cells are also present in medially, between the oculomotor nuclei, dorsally in the supraoculomotor area (SOA) and laterally in the midbrain reticular formation (MRF); and even within the oculomotor nucleus proper. In C&D, a section rostral to the oculomotor and anteromedian nuclei, the urocortin^{+} cells form two columns. Scale bar = 1.0 mm in A&C and 0.5 mm in B&D.

NIH-PA Author Manuscript
NIH-PA Author Manuscript
NIH-PA Author Manuscript

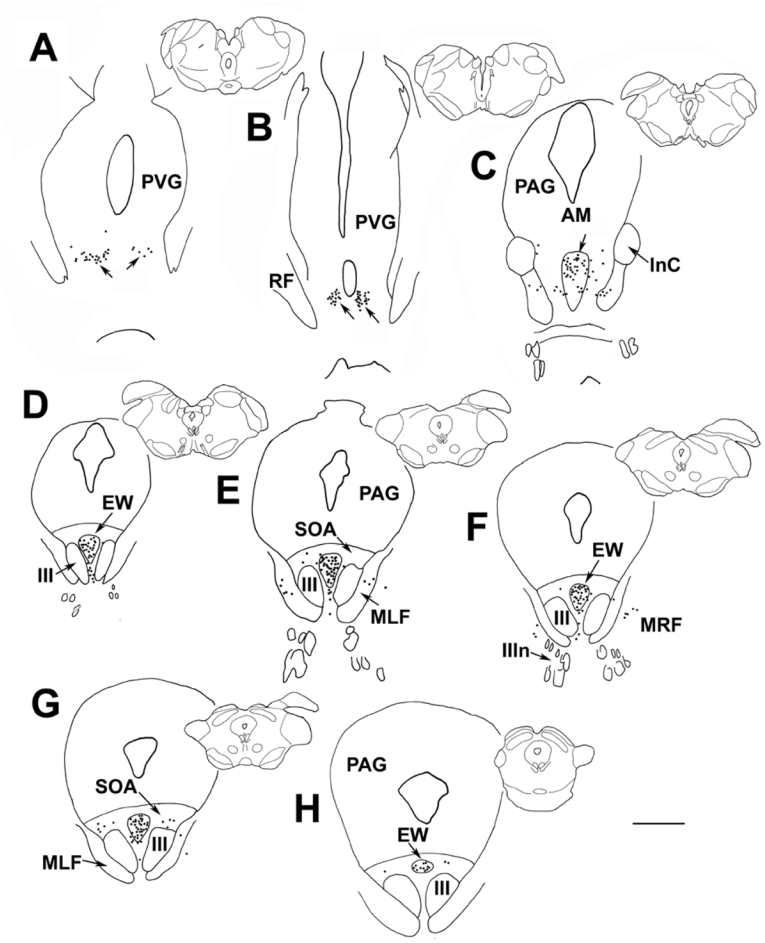

Figure 6.

Rostral (A) to caudal (H) charting of the distribution of urocortin^{+} neurons in the cat perioculomotor region. Urocortin^{+} cells are found within and lateral to the anteromedian nucleus (AM) (C), as well as rostral to it (A&B), where they form two columns. Large numbers of urocortin^{+} cells are also found in the Edinger-Westphal nucleus (EW) at more caudal levels (D–H). Scattered cells are located in the supraoculomotor area (SOA) (E–H), and extend laterally into the medial longitudinal fasciculus (MLF) (D–G) and midbrain reticular formation (MRF) (D–G). Scale bar = 1.0 mm.

NIH-PA Author Manuscript
NIH-PA Author Manuscript
NIH-PA Author Manuscript

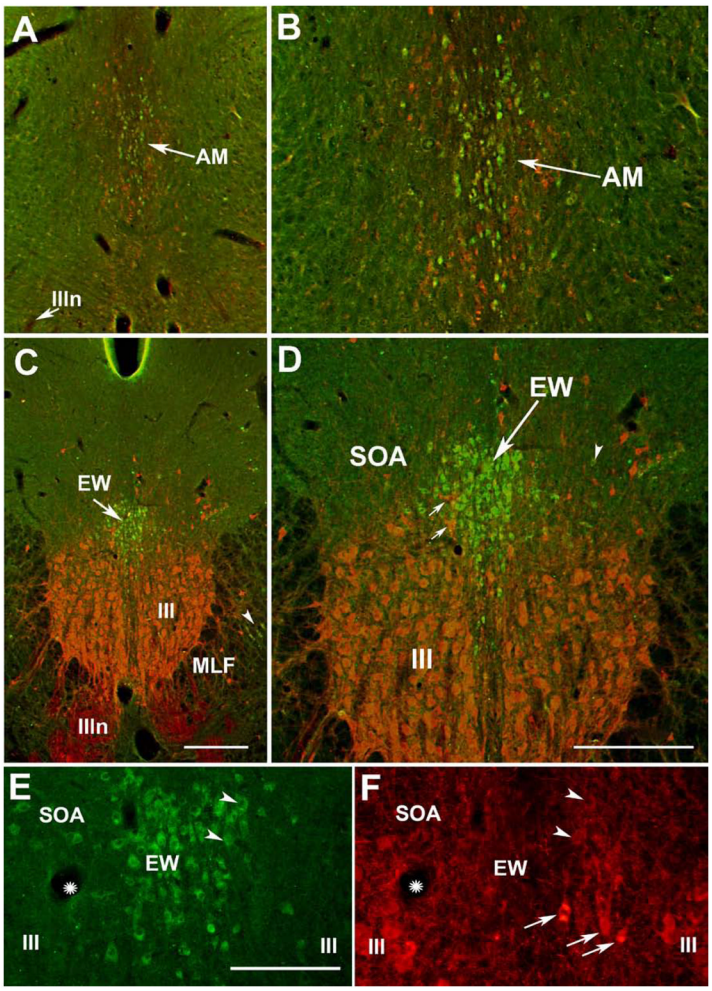

Figure 7.

Fluorescence immunohistochemistry images to simultaneously demonstrate urocortin$^+$ (green) and ChAT$^+$ (magenta) neurons in the cat. B&D show high magnification views of the sections shown in A&C respectively. C&D are from the middle of the oculomotor nucleus (III), while A&B are from the level of AM. Caudally, most ChAT$^+$ cells are found within the oculomotor nucleus (C&D). They are also scattered in the supraoculomotor area (SOA) dorsal to the oculomotor nucleus, and in and ventrolateral to the medial longitudinal fasciculus (MLF). The main body of Urocortin$^+$ cells is contained within the Edinger-Westphal nucleus (EW). Note that a few urocortin$^+$ cells are also present in the SOA and the midbrain reticular formation (arrowheads). Rostrally, the magenta ChAT$^+$ cells are located in and lateral to AM (A&B). The green urocortin$^+$ cells dominate the core of AM, but are also seen lateral to the nucleus. E&F show higher magnification views of the same area of another section as seen through the filters demonstrating the urocortin antibody (green) and ChAT antibody (magenta), respectively. In E, urocortin$^+$ cells fill EW and scattered cells are present in SOA. In F, ChAT$^+$ cells are present in the oculomotor nucleus (III), and a few highly fluorescent ChAT$^+$ cells are located in EW (arrows). Note that some of the urocortin$^+$ cells (E) show low levels of magenta fluorescence (F) (arrowheads). Magnification in A=C, B=D, E=F. Scale bars in C&D = 0.5 mm. [N.B. red has been digitally altered to magenta at the request of the journal.] Scale bar in E = 250 μm.

NIH-PA Author Manuscript
NIH-PA Author Manuscript
NIH-PA Author Manuscript

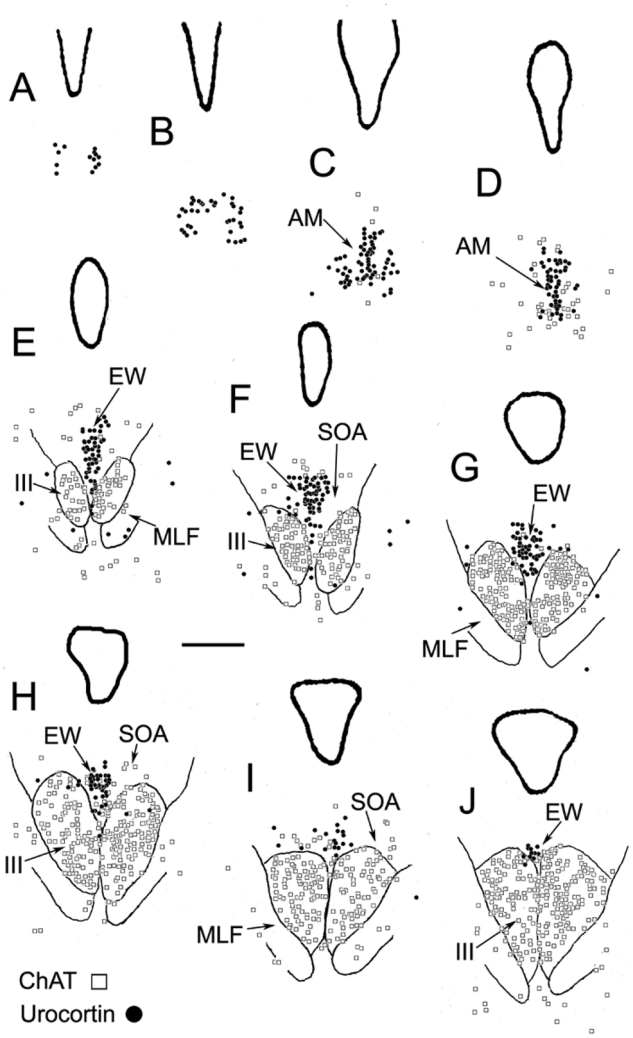

Figure 8.

Charting of the distributions of ChAT$^+$ (Q) and urocortin$^+$ (M) neurons in the cat from double label, fluorescence sections like those illustrated in figure 7. A–I is a rostral to caudal series. As shown in C&D, ChAT$^+$ neurons are found in the anteromedian nucleus (AM) and extend lateral to this nucleus. The urocortin$^+$ cells lie within AM (A–C), and extend into lateral wings, which continue rostrally (A&B) as paired columns. At more caudal levels (D–J), urocortin$^+$ cells are primarily located within the Edinger-Westphal nucleus. However, scattered cells are present ventrally, between the oculomotor nuclei, and laterally, in the supraoculomotor area (SOA). A few even lie in the midbrain reticular formation (MRF). The urocortin$^+$ distribution ends caudal to J, at the level of the caudal central subdivision. Most of the ChAT$^+$ cells are found within the oculomotor nucleus (III). Scattered cells are seen in the SOA, lateral and dorsal to EW, and in and below the MLF. Very few ChAT$^+$ cells are located in the Edinger-Westphal nucleus (EW). Scale bar = 1.0.

NIH-PA Author Manuscript
NIH-PA Author Manuscript
NIH-PA Author Manuscript

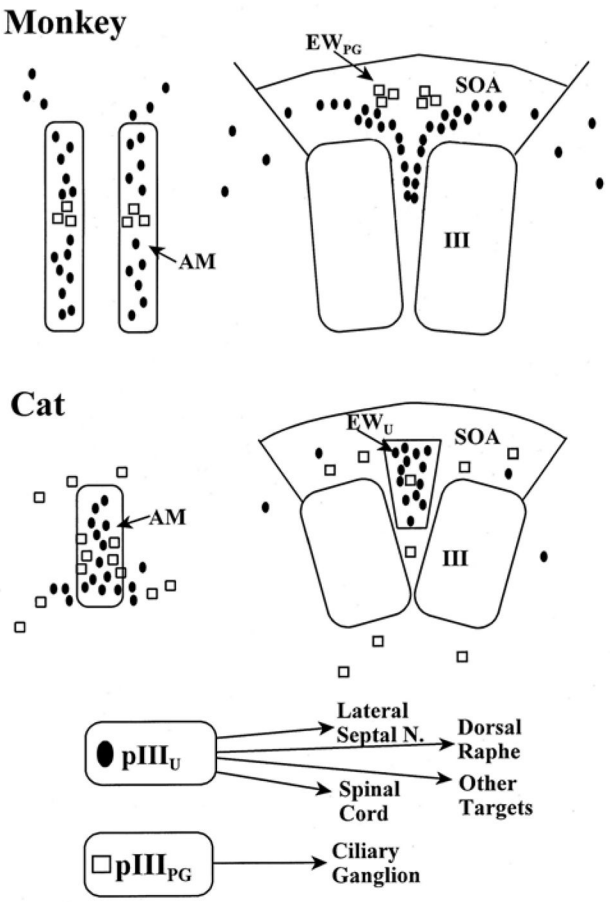

Figure 9.

Schematic diagram showing the distribution for monkey and cat (Above) and known projections (Below) of the perioculomotor urocortin^{+} population (pIII$_{U}$) of cells (M), and the perioculomotor preganglionic motoneurons (pIII$_{PG}$) (G).